CHAPTER 2

POLYETHYLENIMINE (PEI), TETRAHYDROFURAN-HYDROGE PEROXIDE (THF-H_2O_2), AND 2-(3,4-EPOXYCYCLOHEXYL)-ETHYLTRIMETHOXYSILANE (EETMS) MEDIATED SYNTHESIS OF NANOCRYSTALLINE PRUSSIAN BLUE NANOPARTICLES AND THEIR CHARACTERIZATIONS

2.1 Introduction

Prussian blue (PB) and its analogues have been studied extensively over the past decade for their structural, electronic, and magnetic properties, and have been found to function as high-temperature molecular magnets, photo-switchable magnetic solids, antidotes for radioactive poisoning, molecular sieves, electrocatalytic, and hydrogen storage materials (Ding et al., 2009; Entley and Girolami, 1995; Ferlay et al., 1995; Holmes and Girolami, 1999; Kaye and Long, 2005; Sato et al., 1996; Shatruk et al., 2007). As a sensing material, energy storage devices, and a variety of other uses, Prussian blue, and its mixed metal equivalents have become promising tools for the detection of several biological or non-biological analytes (Sattarahmady and Heli, 2011; Yang et al., 2012; You et al., 2014; Zhang et al., 2012). The regulated synthesis of Prussian blue is necessary because, despite its many useful features, its complex structure makes it difficult to determine its exact makeup (Samain et al. 2013). While it is true that all Prussian blues are extremely insoluble (Samain et al. 2013), with a solubility product of ca. 1×10^{-41}, the preparation of water soluble PB is of fundamental and technological interests because they may be easier to manipulate and, consequently, integrate into future molecule-based electronic devices. As a result, stabilized Prussian blue nanoparticles (PBNPs) have been developed in an effort to control Prussian blue nucleation and prevent extensive networks (Pandey and Pandey, 2013c). Previously, it was shown that the single precursor potassium ferricyanide [K_3 {Fe $(CN)_6$}] can be converted into processable PBNPs using 3-aminopropyltrimethoxysilane (3-APTMS) and cyclohexanone, with an average particle size on the order of 15.6 nm, which is sufficient to explain the remarkable electron transfer rate constant [32.1 s^{-1}] (Pandey and Pandey, 2013c). The controlled synthesis of mixed-metal compounds with super peroxidase mimetic activity was accomplished in the same

way (Pandey and Pandey 2013d). However, the practical usability of the nanomaterial in question was reduced due to the use of 3-APTMS during the operation and processing of PBNPs, prompting a search for a suitable substitute of 3-APTMS. These additional problems were linked to auto hydrolysis, condensation, and polycondensation of the alkoxy group.

We were very fortunate in that we were able to successfully replace 3-APTMS with tetrahydrofuran-hydroperoxide (THF-H_2O_2), which effectively facilitated the conversion of K_3[Fe $(CN)_6$] into water-soluble PBNPS under ambient conditions (Pandey and Pandey, 2014a). Tetrahydrofuran (THF) and hydrogen peroxide (H_2O_2) were again used in the synthesis of PBNPs, which prompted us to assess their contributions. In the presence of THF and H_2O_2 at 60 °C, it was discovered that K_3[Fe $(CN)_6$] underwent regulated conversion into water-soluble PBNPs after three hours (Pandey and Panday, 2016b).

Polyethylenimine (PEI) has recently been shown to play a key role in transforming double precursors into Prussian blue Nanocubes. In an acidic solution comprising PEI, $FeCl_3$, K_3[Fe $(CN)_6$], and KCI (Zhai et al., 2008), Prussian Blue Nanocubes were fabricated with an edge length of 50 nm and a uniform size. Because of the difficulties in processing double precursors for electroanalytical uses, we set out to synthesize water-soluble PBNPs with the help of PEI from the single precursor K_3[Fe $(CN)_6$]. The Prussian blue created using the traditional way of chemical synthesis is insoluble in many solvents, limiting its use in a variety of practical applications. Accordingly. One difficult task has been to develop a controlled synthetic approach that results in the creation of Prussian blue nanoparticles (PBNPs).

From a practical standpoint, the MHCF's size is crucial. The dispersibility of these MHCFs in a given solvent is enhanced by shrinking to sub-nanometer dimensions. It's useful for studying electrochromic behavior, making composites, and processing materials into thin films. Prussian blue nanoparticles (PBNPs) of various sizes and shapes can be synthesized in a controlled manner by adjusting the molar ratio of protection to the precursor (Durand et al., 2010; Johansson et al., 2005; Uemura and Kitagawa, 2003). Important in developing nanoparticle qualities as a function of size (Fernandez et al., 2010; Shen et al., 2009; Sun et al., 2005; Uemura et al., 2004), is the control over particle shape and size during PB synthesis.

The removal of cesium ions by using incorporating MHCFs within porous matrices like calcium alginate beads and silica alginate beads has already been studied by several authors (Vipin et al., 2013; P.C. Pandey et al., 2018). Porous calcium alginate beads are effective at entrapping larger PB particles, while smaller particles (1-20 nm) may be leached out in the field. For this reason, it could be useful to fine-tune the porous morphology of calcium alginate beads in such a way that they can accurately encapsulate tiny PBN within the porous matrix, so making it appropriate for possible medicinal applications. In combination with a calcium alginate precursor, alkoxysilanes containing R-Si(OR)$_3$ can generate Si-O-Si- linkage within the alginate's porous matrix, potentially resulting in the creation of silica-alginate beads. The current study reports an innovation along these lines that justifies the use of 2-(3,4-epoxycyclohexyl)-ethyltrimethoxysilane (EETMS), another functional alkoxysilane. The regulated conversion of potassium hexacyanoferrate into PBN is discovered to be made possible by EETMS.

The present finding elaborates the synthesis of PBNPs through PEI, THF-H_2O_2, and EETMS that provide the facile and size-controlled synthesis. Moreover, removal of hazardous material, the mesoporous matrix like silica (SiO_2) is suitable for the encapsulation of PBNPs. The findings on these lines are reported in this investigation.

2.2 Experimental Section

2.2.1 Materials

2-(3,4-epoxycyclohexyl)-ethyltrimethoxysilane (EETMS), and cyclohexanone were obtained from PubChem. Polyethylenimine (PEI) (mol. Wt. 60,000), graphite powder (particle size 1-2 μm), and nujol oil were purchased from Sigma-Aldrich Chemical Co., India. Cesium chloride, tetrahydrofuran, and hydrogen peroxide were purchased from Sisco Research Laboratories Pvt. Ltd. (Mumbai, Maharashtra, India). Potassium ferricyanide was obtained from Millipore Sigma India (Bengaluru, Karnataka, India). The remaining chemicals were purchased from commercial sources Sigma Aldrich India and were of analytical grade. Milli-Q water was used throughout the experiment to avoid interference from contaminants.

2.2.2 Polyethylenimine (PEI) mediated synthesis of nanocrystalline (PBNP-1)

200 μl aqueous solution of $K_3[Fe(CN)_6]$ (0.05M) and 65 μl of PEI (0.15mg/ml) were mixed under stirred conditions over a vertex cyclomixer followed by the addition of 10 μl HCl (6.5 M). The resultant mixture was kept at 60 ^{0}C in an oven for 5 hours. The yellow-color solution turned into a deep blue color which indicated the formation of PBNP-1 having absorption maxima at 680 nm.

2.2.3 THF-H_2O_2 mediated synthesis of nanocrystalline (PBNP-2)

200 µl aqueous solution of $K_3[Fe(CN)_6]$ (0.05M) and 65 µl of THF (12 M) were mixed under stirred conditions over a vertex cyclomixer and 130 µl of H_2O_2 (0.7 M). The resultant mixture was kept at 60 ^{0}C for 2 hours in the oven. The yellow-colored solution of $K_3[Fe(CN)_6]$ was turned into a deep blue color solution indicating the conversion of a single precursor into PBNP-2.

2.2.4 2-(3,4-Epoxycyclohexyl)-ethyltrimethoxysilane (EETMS) and cyclohexanone mediated synthesis of nanocrystalline (PBNP-3)

100 µl aqueous solution of $K_3[Fe(CN)_6]$ (0.02M) and 20 µl of EETMS (0.2M) were mixed under stirred conditions over a vertex cyclomixer followed by drop-wise addition of 12 µl cyclohexanone (9.62M). The resultant mixture was kept at 60 ^{0}C for 3 hours in the oven. The yellow-colored solutions were turned into deep blue-colored solutions indicating the formation of PBNP-3.

2.2.5 THF-H_2O_2 mediated synthetic incorporation of nanocrystalline (PBNP) within MSP and Mesoporous silica nanoparticles (MSNP) as potential Cesium ion Adsorbent:

120 mg MSN was suspended in 300 µl $K_3[Fe(CN)_6]$ (0.65M) and mixed over cyclomixer for 3 hours followed by the collection of potassium hexacyanoferrate inserted MSN by centrifugation. Potassium hexacyanoferrate inserted MSN were suspended into a reaction mixture containing 170

μl of THF (12 M) and 340 μl of H_2O_2 (0.7 M) under stirring over cyclomixer and allowed to stand for 1.5 hours followed by incubation in the oven at 65 ^{0}C for 6-7 hours. The yellow-color MSN was turned into deep blue color indicating the conversion of MSN-inserted potassium hexacyanoferrate to Prussian blue nanoparticles within the mesoporous matrix. As made PBNP within MSN was stirred under ambient conditions over cyclomixer for 30 min and PBNP inserted MSN were collected by centrifugation followed by washing with Double Distilled Water and collection of PBNP inserted MSN by centrifugation until blue color supernatant becomes colorless. A similar procedure was adopted for the synthetic insertion of PBNP with Mesoporous silica nanoparticles of an average size of 200 nm.

2.2.6 Preparation of Prussian blue nanoparticles modified screen-printed electrode

The screen-printed electrode was freshly prepared in a three-electrode configuration was developed using silver, graphite, and Ag/AgCl pastes as shown below via screen printing technology; graphite was used for the working and counter electrodes, Ag/AgCl was used for the reference electrode. The working electrode track of the freshly prepared SPE was further modified with a Nordson dispenser using PB nanoparticle printing ink and dried at 380K, 1h for subsequent electrochemical sensing of cesium ions.

2.2.7 Preparation of PBNP-modified graphite paste electrode

The active PBNP-1, PBNP-2, and PBNP-3 modified graphite paste was made by mixing PBNP-1/PBNP-2/PBNP-3, graphite powder, and nujol oil. The process of paste fabrication involves

mixing of 5 µl of PBNP-1/PBNP-2/PBNP-3 with 9 mg spectroscopic grade graphite powder, under sonication for 30 min followed by drying the same at 60 ^{0}C in a vacuum oven overnight. Active PBNP-modified graphite paste was made by mixing graphite powder= 68% (w/w), PBNP adsorbed graphite= 2.5% (w/w) and nujol oil = 30% (w/w) The electrode body has a well of the recessed depth of 2 mm was filled with an active paste. The paste surface was manually smoothed on clean butter paper.

Table 2.1. Characteristics of PBNP-1 as a Function of PEI Concentration

Vial	$K_3[Fe(CN)_6]$ (mol L^{-1})	PEI (mg/mL)	HCl (mol L^{-1})	PBNPs Sol. Color	Extent of Formation
A	0.05	0.10	6.5	Light Blue	+
B	0.05	0.15	6.5	Dark Blue	+++
C	0.05	0.20	6.5	Light Blue	++
D	0.05	0.25	6.5	Greenish Blue	-

Table 2.2. Characteristics of PBNP-1 as a function of $K_3[Fe(CN)_6]$ Concentration

Vial	$K_3[Fe(CN)_6]$ (mol L^{-1})	PEI (Mg/mL)	HCl (mol L^{-1})	PBNPs Sol. Color	Extent of Formation
A	0.010	0.15	6.5	-ve	-
B	0.025	0.15	6.5	Light Blue	+
C	0.035	0.15	6.5	Blue	++
D	0.050	0.15	6.5	Dark Blue	+++
E	0.060	0.15		Greenish Blue	-

Table 2.3. Characteristics of PBNP-2 as a Function of H_2O_2 Concentration

Vial	$K_3[Fe(CN)_6]$ (mol L^{-1})	THF (mol L^{-1})	H_2O_2 (mol L^{-1})	PBNPs Sol. Color	Extent of Formation
A	0.05	12	0.06	Green	+
B	0.05	12	0.13	Light Blue	++
C	0.05	12	0.35	Light Blue	+++
D	0.05	12	0.70	Blue	+++++
E	0.05	12	1.05	Blue	+++
F	0.05	12	1.40	Light Blue	++

Table 2.4. Characteristics of PBNP-2 as a function of THF Concentration

Vial	$K_3[Fe(CN)_6]$ (mol L^{-1})	THF (mol L^{-1})	H_2O_2 (mol L^{-1})	PBNPs Sol. Color	Extent of Formation
A	0.05	2	0.7	Light Green	+
B	0.05	5	0.7	Light Blue	++
C	0.05	7	0.7	Light Blue	+++
D	0.05	10	0.7	Light Blue	+++
E	0.05	12	0.7	Blue	+++++

Table 2.5. Characteristics of PBNP-2 as a function of $K_3[Fe(CN)_6]$ Concentration

Vial	$K_3[Fe(CN)_6]$ (mol L^{-1})	THF (mol L^{-1})	H_2O_2 (mol L^{-1})	PBNPs Sol. Color	Extent of Formation
A	0.015	12	0.7	-ve	-
B	0.025	12	0.7	Light Blue	++
C	0.03	12	0.7	Light Blue	++
D	0.04	12	0.7	Light Blue	+++
E	0.05	12	0.7	Blue	+++++
F	0.06	12	0.7	Light Blue	++

Table 2.6. Characteristics of PBNP-3 as a function of EETMS Concentration

Vial	$K_3[Fe(CN)_6]$ (mol L^{-1})	EETMS (mol L^{-1})	Cyclohexanone (mol L^{-1})	PBNPs Sol. Color	Extent of Formation
A	0.02	0.05	9.6	-ve	-
B	0.02	0.08	9.6	Greenish Blue	+
C	0.02	0.2	9.6	Blue	++++
D	0.02	0.3	9.6	Light Blue	++

Table 2.7. Characteristics of PBNP-3 as a function of $K_3[Fe(CN)_6]$ Concentration

Vial	$K_3[Fe(CN)_6]$ (mol L^{-1})	EETMS (mol L^{-1})	Cyclohexanone (mol L^{-1})	PBNPs Sol. Color	Extent of Formation
A	0.005	0.2	9.6	-ve	-
B	0.01	0.2	9.6	Light Blue	++
C	0.02	0.2	9.6	Blue	++++
D	0.03	0.2	9.6	Greenish Blue	+

2.3 Characterization of synthesized nanocrystalline PBNP

The UV-visible absorption spectra of PBNP were recorded using a Hitachi U-2900 spectrophotometer. TEM analysis was performed using Tecani G2 20 TWIN (USA). The morphological characteristics of synthesized PBNP over SiO_2, were analyzed using FE-SEM (Scanning electron microscopy) of FEI Company of USA (SEA), PTE LTD. Energy dispersive spectrometer (EDS) for elemental conformation and mapping was accomplished with Nova Nano SEM 450 (USA). X-ray diffractometer (Rigaku Miniflex 600 Desktop X-Ray Diffraction System, Japan) was used to examine the diffractogram of the PBNPS in the scanning range between 10-90^0. The sample was prepared for Zeta potential analysis by diluting corresponding nanoparticles done with Zetasizer nano ZS90 (Malvern instrument). Thermogravimetric analysis of the PBNPs was performed by TGA-50 M/s Shimadzu (Asia Pacific) Pte Ltd which shows the water loss in the sample. Electrochemical experiments like- cyclic voltammetry (CV), and differential pulse voltammetry (DPV), were performed on an electrochemical workstation model CHI660B, CH Instrument Inc., TX, i.e., a three-electrode configuration with a working volume of 3 ml. The electrode body has been purchased from Bioanalytical systems. Platinum and Ag/AgCl wire are served as counter electrode and reference electrode, respectively. The working electrode is PBNPs modified carbon paste electrode (CPE). The active paste of PBNPs was synthesized by mixing 50 µl of PBNP suspension with 65 mg graphite powder (spectroscopic grade, 1-2 µm) followed by ultrasonication and left to dry in a vacuum oven for overnight at 65 ^{0}C. The composition of the working electrode is graphite powder = 68% w/w, nujol oil = 28% w/w, and PBNP = 4% w/w.

2.3.1 UV-Visible spectrophotometer

The UV spectrophotometer shows the absorbance of potassium ferricyanide, and before the synthesis of PBNP-1, PBNP-2, and PBNP-2 at 420 nm, respectively, but after the synthesis of PBNP-1, PBNP-2, and PBNP-3 peaks obtained at 680 nm (Fig. 2.1). Similarly, the successful conversion of $K_3[Fe(CN)_6]$ to PB was achieved by the chemical reduction approach by altering one component while keeping the other component unchanged (Table 2.1–2.7). Based on UV-Vis. Spectra, conversion of potassium hexacyanoferrate to PBNPs was estimated between 55% - 95%.

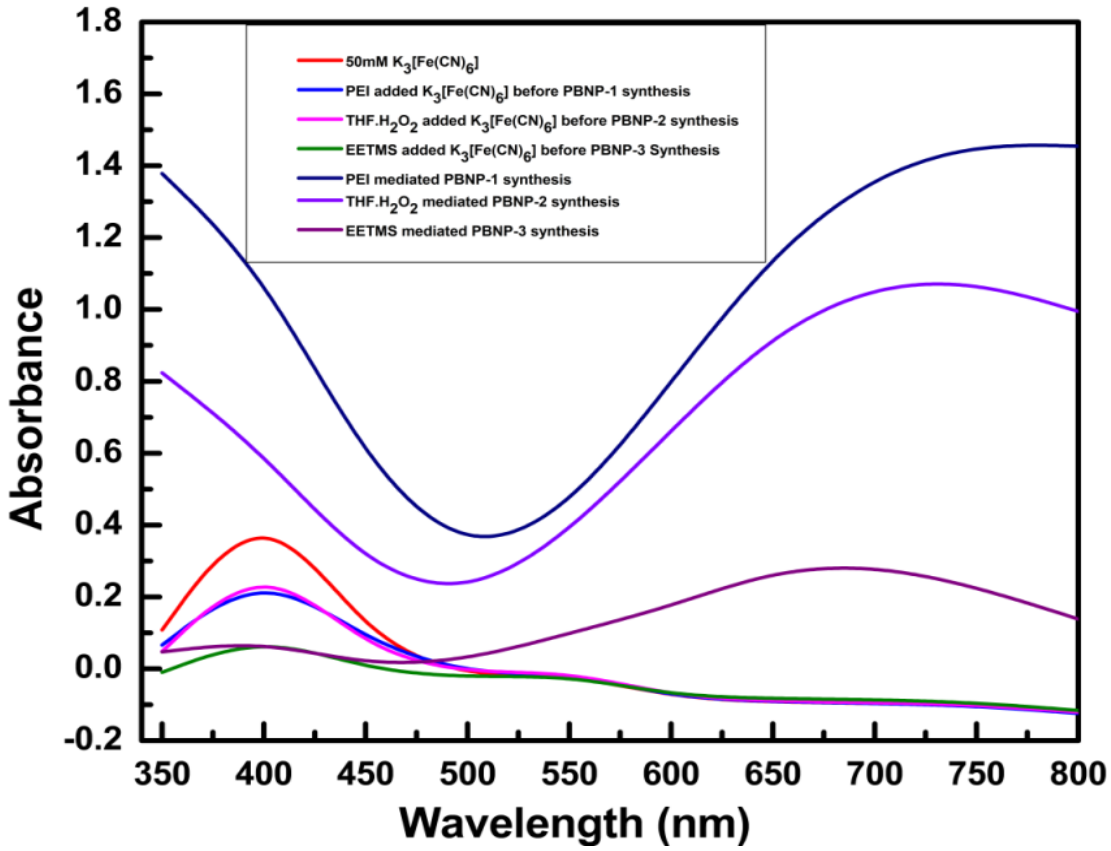

Figure 2.1. UV-Vis. spectra of recorded potassium ferricyanide, before and after synthesis of PBNP-1, PBNP-2, and PBNP-3.

2.3.2 Powder X-ray diffraction (XRD)

Powder X-ray diffraction analysis has shown that as-prepared PBNP is crystalline. The sharp peak indexed at 2θ values of PBNP-1 17.4º, 24.96º, 35.43º, 39.5º, 50.72º, 53.9º and 57.2º (Fig. 2.2a); PBNP-2 17.4º, 24.96º and 35.43º (Fig. 2.2b); PBNP-3 17.4º, 24.96º, 35.43º and 50.72º (Fig. 2.2c); and for PBNP-2@MSNP 17.4º, 24.7º, 35.3º, 39.6º, 43.7º, 50.0º, 53.9º, 57.2º, 66.1º, 68.9º and 77.2º (Fig. 2.2 d). All PBNP peaks assigned to (200), (220), (400), (420), (422), (440), (600), (620), (640), (642), and (820) planes show face-centered cubic lattice type structure (JCPDS no. 73-0687).

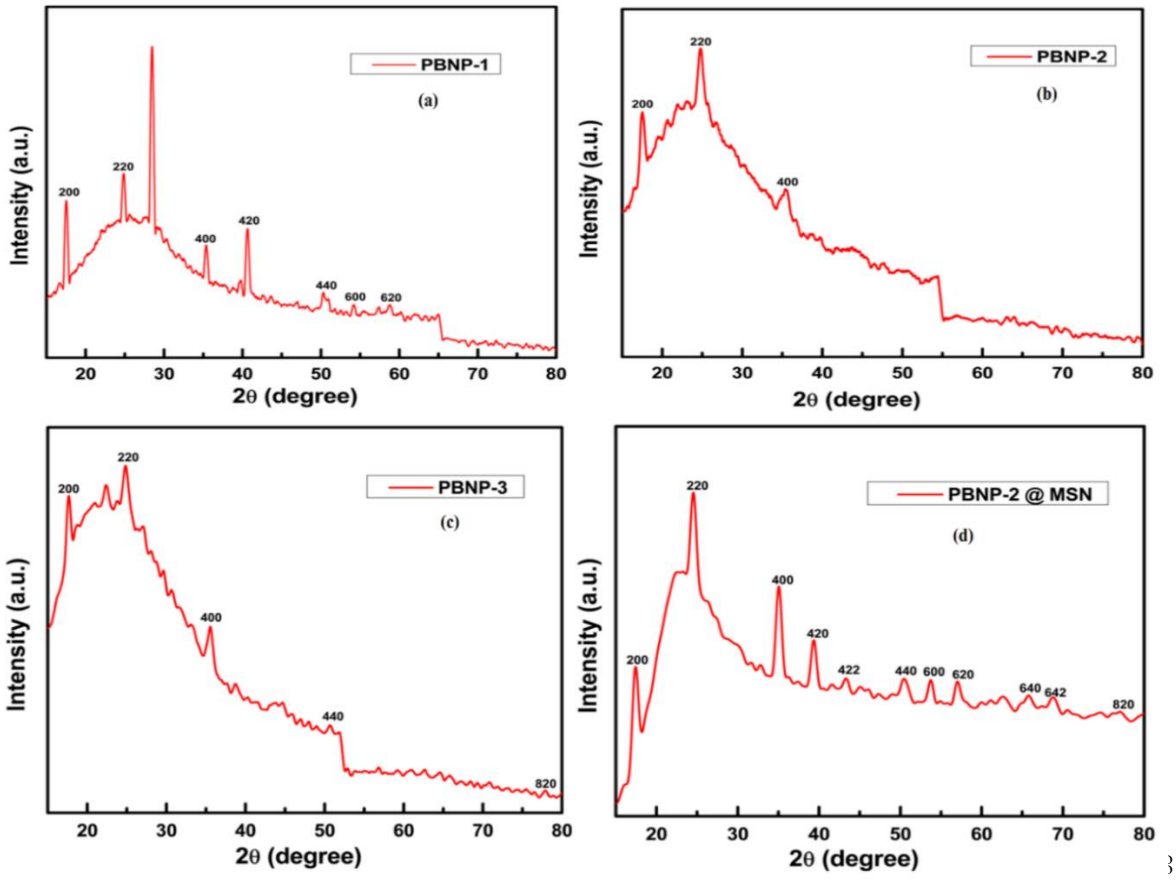

Figure 2.2. XRD of PBNP-1 (a), PBNP-2 (b), PBNP-3 (c), and PBNP-2@MSN (d).

Using Scherrer's equation, the crystalline sizes for PBNP-1, PBNP-2, PBNP-3, and PBNP-2@MSN were determined to be 35.8 nm, 43.8 nm, 39.5 nm, and 6.0 nm, respectively. Since, the XRD of PBNPs thin film made on a glass surface was recorded, the diffractograms as shown in Figure 2.2(a-c) also justified the presence of silica as evidence of a plateau indexed at 2θ values between 20-25. The XRD of heterogeneous PBNP (PBNP-2@MSN) inserted within mesoporous silica was recorded in powdered form. PBNP-2 and PBNP-3 are less crystalline compared to PBNP-1 and PBNP-2@MSN because due to the presence of a high concentration of organic moiety (like- THF-H_2O_2, EETMS) whereas PBNP-1 incorporates polycationic polymer (PEI) with less organic residue and PBNP-2@MSN incorporated with silica nanoparticle that is polycrystalline in nature (P.C. Pandey et al., 2016c; P.C. Pandey et al., 2018).

2.3.3 SEM analysis of synthesized PBNP@MSN (Mesoporous silica nanoparticles)

Scanning electron microscopy (SEM) was used to determine the dimensions and morphology of the synthesized PBNP@MSN. Microporous (6.1Å) and mesoporous (63.54Å) arrangements on the surface of MSN have been described (Dutta et al., 2005). Fig. 2.3a displays the results of an HRSEM study showing the heterogeneously dispersed nanosphere of PBNP implanted on MSN.

EDX spectrum shows the stronger peak of PBNP@MSN confirming the presence of all elements such as Si and Fe i.e., the main component (Fig. 2.3b). The synthesized PBNP@MSN revealed the weight percentage at 94.49 % of Si and 5.51 % of Fe in the EDX spectrum for the corresponding sample.

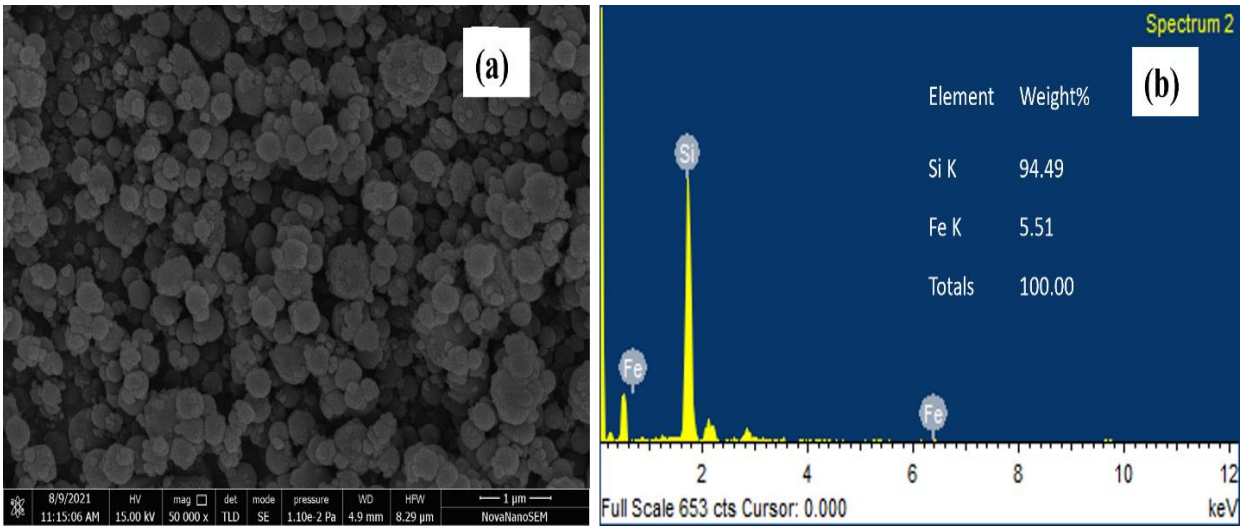

Figure 2.3. HR-SEM of PBNP@MSN confirmed the successful synthesis of PBNP over MSN (a), and the EDX spectrum showed the presence of mandatory elements (b).

2.3.4 TEM analysis

TEM characterization of as-made PBNPs confirmed the size and shape as shown in Figures 2.4, 2.5, and 2.6. The shape PBNP-1 is spherical (Fig. 2.4a), whereas PBNP-2 (Fig. 2.5a), and PBNP-3 (Fig. 2.6a) are rectangular. The SAED (selected area electron diffraction) pattern displays the non-crystalline nature of PBNP-1 (Fig. 2.4b) and PBNP-3 (Fig. 2.6b) attributed to the presence of cationic polymer and silane, respectively. While the polycrystalline nature of PBNP-2 could be due to THF (Fig. 2.5b). The resulting histogram displayed well-distributed particles of PBNP-1, PBNP-2, and PBNP-3, and the average size for PBNP-1 ~6 nm (Fig. 2.4c), PBNP-2 ~59 nm (Fig. 2.5c) and, PBNP-3 ~28 nm (Fig. 2.6c) respectively.

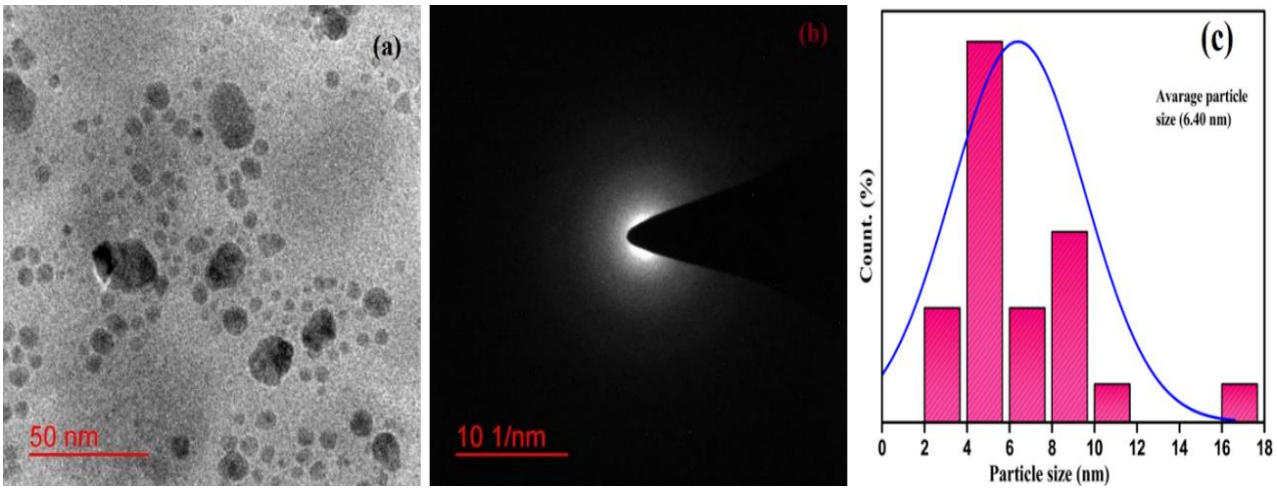

Figure 2.4. TEM image of PBNP-1 (a), SAED pattern (b), and bar histogram displaying the particle size distribution of corresponding nanoparticles (c).

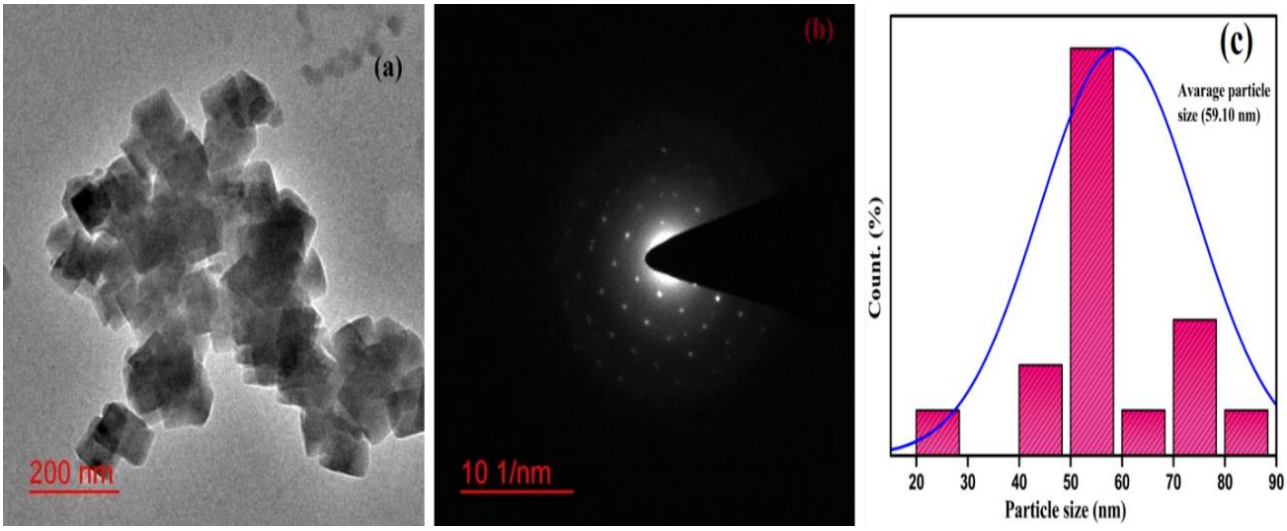

Figure 2.5. TEM image of PBNP-2 (a), SAED pattern (b), and bar histogram displaying the particle size distribution of corresponding nanoparticles (c).

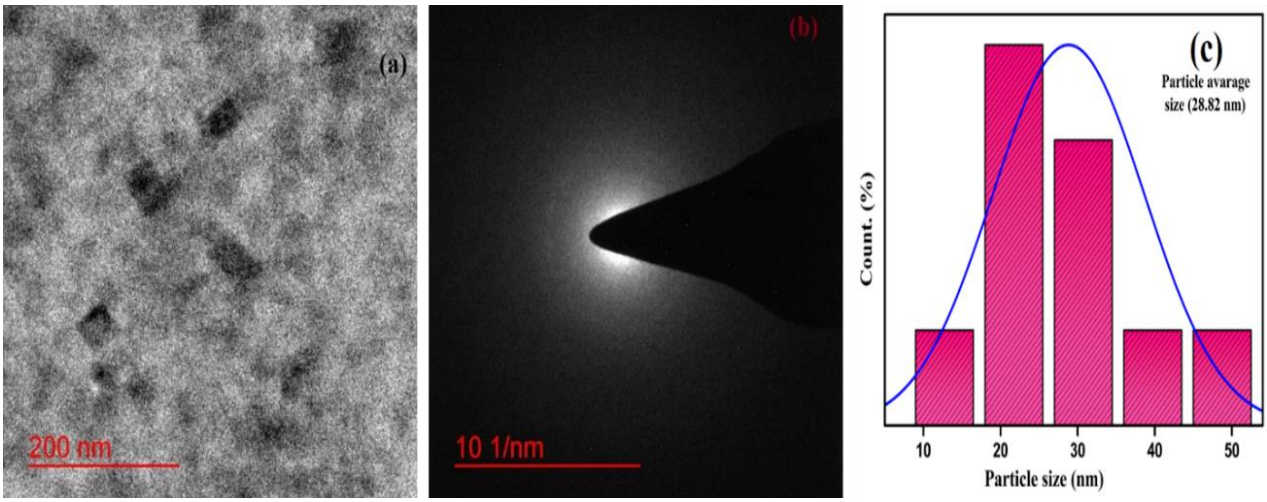

Figure 2.6. TEM image of PBNP-3 (a), SAED pattern (b), and bar histogram displaying the particle size distribution of corresponding nanoparticles (c).

2.3.5 DLS Characterization of Nanoparticles

The zeta potential of nanoparticles was measured as 51.6 ± 3 mV, -26.6 ± .1 mV, and -34.1, ± 2.2 mV (as shown in Fig. 2.7 a,b,c) for PBNP-1, PBNP-2, and PBNP-3 respectively corresponds to their charged surface.

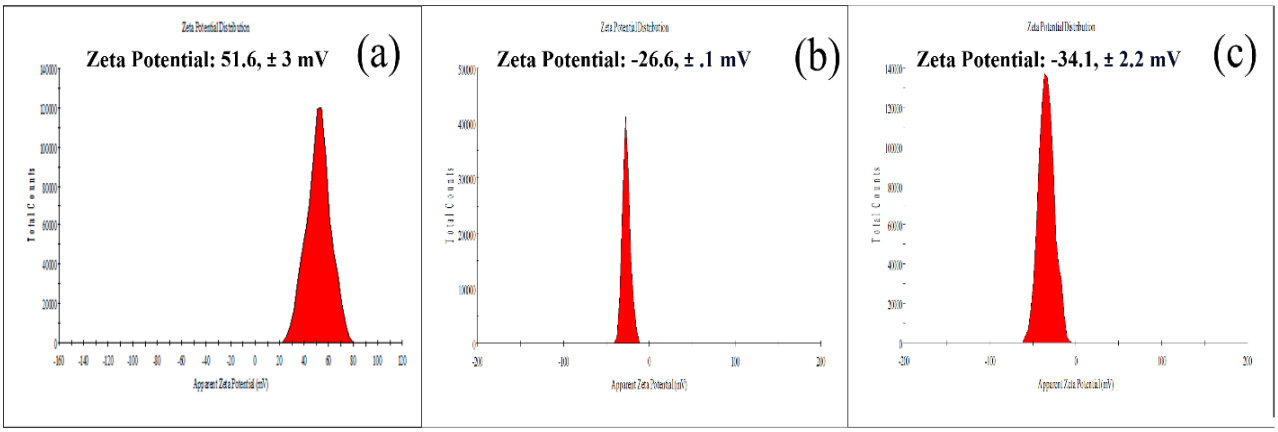

Figure 2.7. DLS characterization for zeta potential of PBNP-1 (a), PBNP-2 (b), and PBNP-3 (c).

2.3.6 Thermogravimetric (TGA) analysis

Prussian blue PBNP-1, PBNP-2, and PBNP-3 thermogravimetric analysis (TGA) profiles are depicted in Figure 2.8. TGA analysis was used to assess the thermal stability of the manufactured Prussian blue nanoparticles. Most of the time, weight loss during thermogravimetric analysis is performed to investigate the presence of nanoparticles in nanomaterials. Because catalyst particles were present during the weight loss analysis, and it is not easy to interpret these data. The temperature at which Prussian blue nanoparticles oxidized is an indication of its stability. TGA graph shows four regions for PBNP-1, three regions for PBNP-2, and PBNP-3 where the PB has lost weight (Fig. 2.8 a,b,c). Weight loss in PBNP-1(Fig. 2.8a) began around 100 °C and ended at 245 °C, in PBNP-2 (Fig. 2.8b) it began at 140 °C and ended at 288 °C, and in PBNP-3 (Fig. 2.8c) it began at 235 °C and ended at 405°C, this may be due to the elimination of water molecules that had been absorbed by the Prussian blue moiety. The second and third weight losses for PBNP-1, PBNP-2, and PBNP-3 at temperatures ranging from 260 °C to 430 °C, 312 °C to 477 °C, 425 °C to 572 °C, and 441 °C to 554 °C, 482 °C to 713 °C, 592 °C to 700 °C, respectively, and fourth weight loss for PBNP-1 is at between 562 °C to 774 °C are moderated and could be attributed to the presence of soluble and insoluble Prussian blue nanoparticles. PBNP-1 mass decreases at steps I, II, III, and IV result in weight losses of 3.73%, 10.77%, 0.92%, and 0.94%, respectively; PBNP-2 mass decreases at steps I, II, and III result in weight losses of 2.30%, 3.74%, and 1.71%, respectively; and PBNP-3 mass decreases at steps I, II, and III result in weight losses of 0.53%, 0.34%, and 0.22%, respectively. The loss of water from the PB structure was thought to be the cause of the mass reductions that occurred in step I. Subsequently, mass reductions occurred in

steps II, III, and IV and were found to be connected with the release of cyanide groups from the PB structure.

2.3.7 BET analysis

The precise surface area and pore diameter of the catalyst as it was created were thoroughly evaluated using BET analysis. Figure 2.8 (d) displays the N_2 adsorption-desorption isotherms for PBNP-2 incorporated mesoporous silica. The adsorption-desorption curve shows that the PBNP-infused mesoporous substrate exhibits a type-IV isotherm with a specific surface area of 40.3 m^2/g and a pore diameter of 7.14 nm. These results clearly show that controlling the nanoscale of chemically synthesized Prussian blue of PBNP-2 incorporated mesoporous silica support for subsequent removal applications.

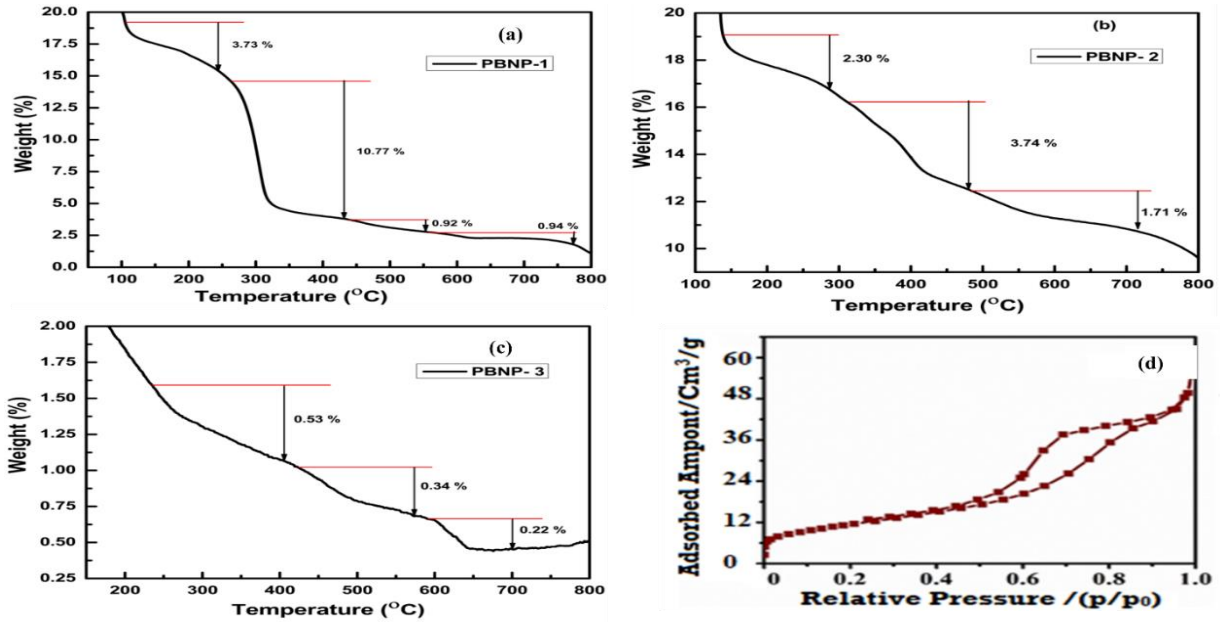

Figure 2.8. TGA analysis of synthesized PBNPs: (a) PBNP-1; (b) PBNP-2 and (c) PBNP-3; (d) N_2 adsorption-desorption isotherms of PBNP-2 inserted mesoporous silica particle.

2.3.8 XPS of PBNP-1, PBNP-2 and PBNP-3

XPS analysis was conducted on PBNP-1, PBNP-2, and PBNP-3 under ambient conditions. Analysis of the XPS data indicated the existence of both Fe (II) and Fe (III) species in the PBNPs samples that were synthesized. The binding energies of PBNP-1, PBNP-2, and PBNP-3 are measured to be 721.04 eV and 707.89 eV, 721.29 eV and 708.25 eV, and 721.18 eV and 708.25 eV, respectively; these values correspond to the Fe 2p1/2 and Fe 2p3/2 orbitals. The observed peaks serve as empirical support for the existence of the distinctive Fe^{2+} moiety within Prussian blue. Furthermore, the identification of peaks at binding energies (BE) of 712.82 eV for PBNP-2, 711.87 eV for PBNP-2, and 712.25 eV for PBNP-3 provide evidence for the existence of Fe^{3+} entities. The X-ray photoelectron spectroscopy (XPS) analysis of all three PBNPs demonstrates that PBNP-1 exhibits a noticeably higher intensity in comparison to PBNP-2 and PBNP-3 (as seen in Figure 2.9 (A-C)).

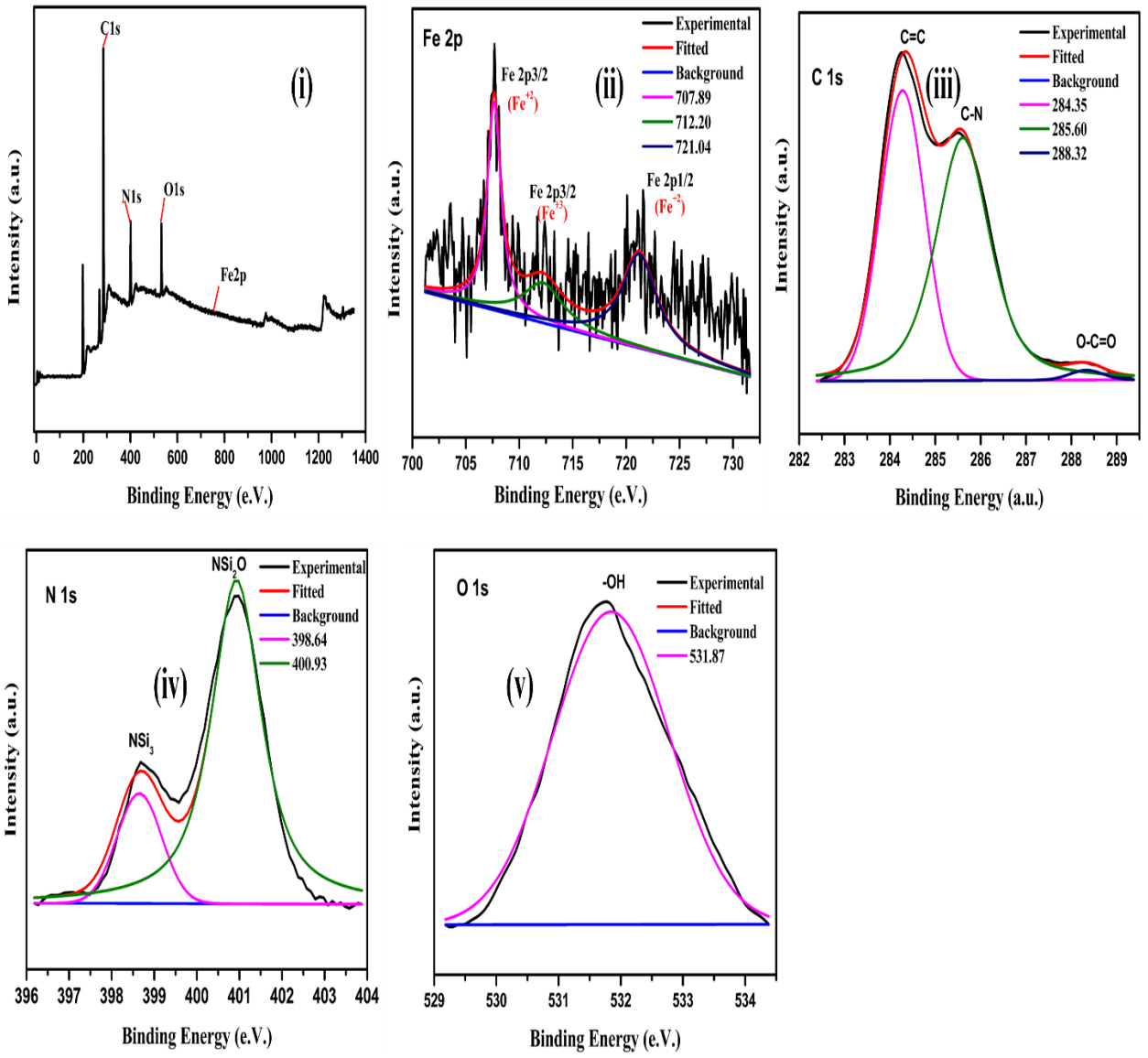

Figure 2.9 (A). Representing the XPS characterization of PBNP-1; (i) elemental scanning; (ii) Fe2p; (iii) C1s; (iv) N1s; (v) O1s.

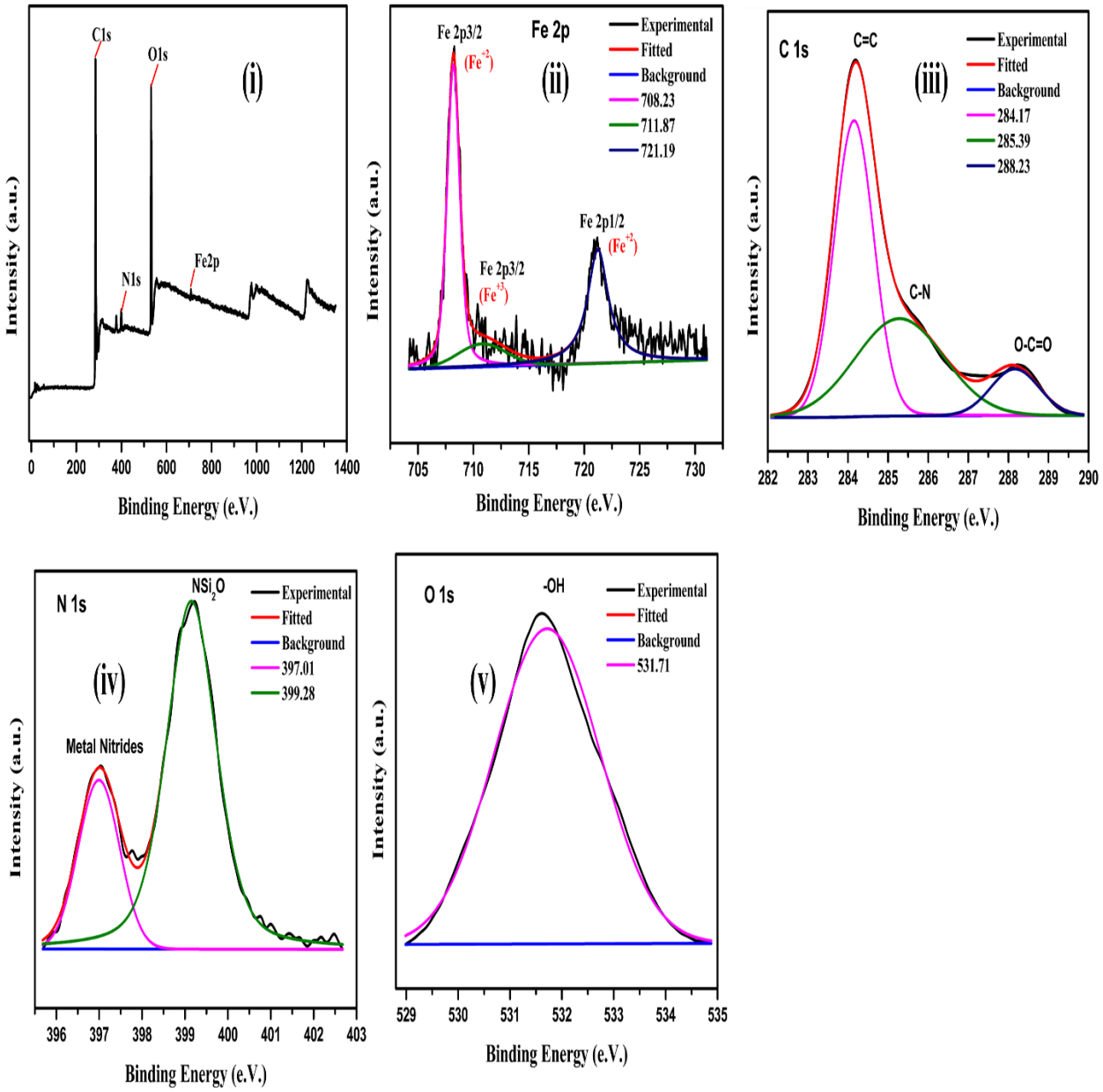

Figure 2.9 (B). Representing the XPS characterization of PBNP-2; (i) elemental scanning; (ii) Fe2p; (iii) C1s; (iv), N1s; (v), O1s.

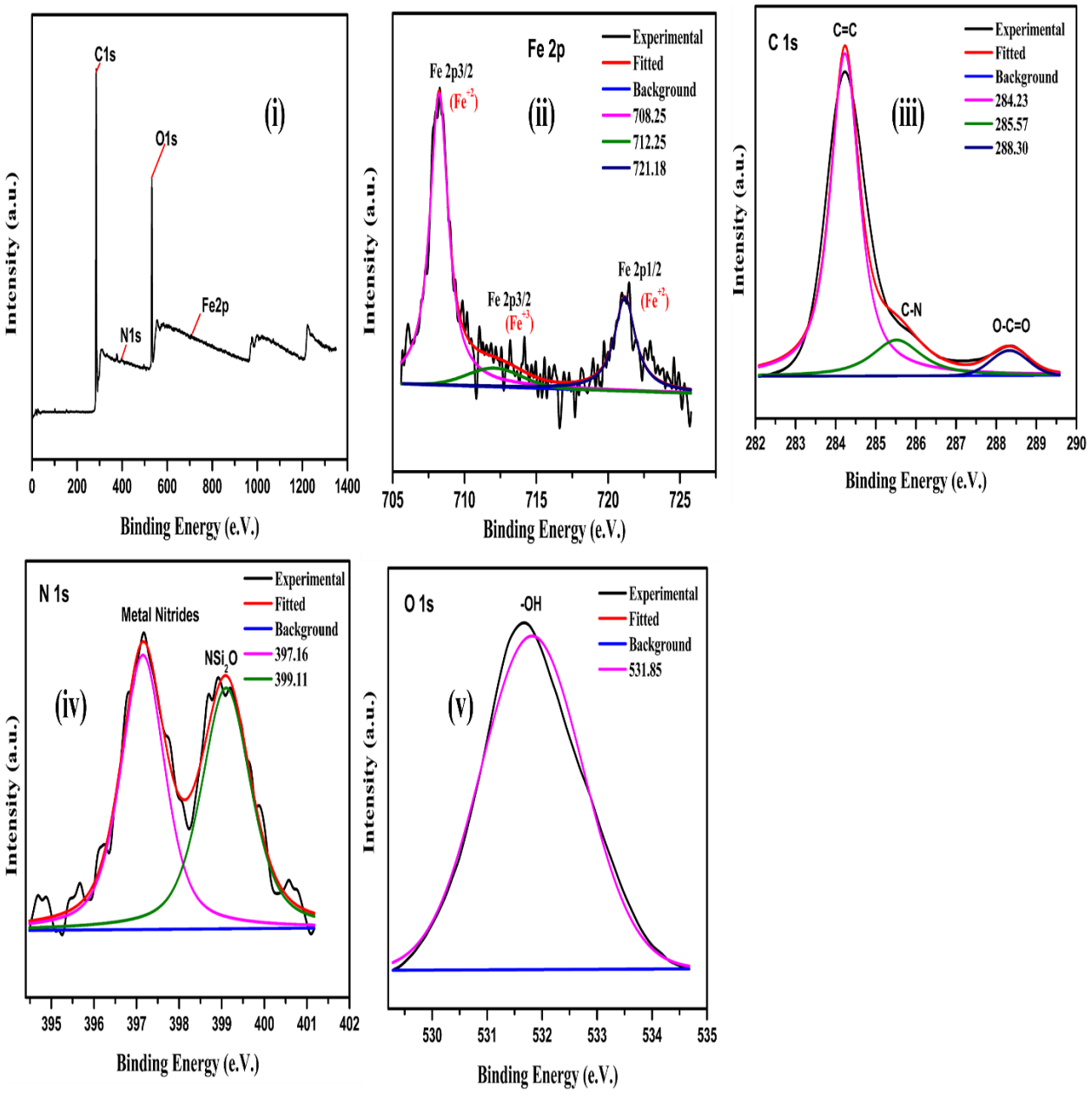

Figure 2.9 (C). Representing the XPS characterization of PBNP-3. (i) elemental scanning; (ii) Fe2p; (iii) C1s; (iv) N1s; (v) O1s.